- Technical Paper -

Numerical Investigation of Effects of Material Properties on Corrosion-induced Concrete Crack Propagation

Di QIAO[*1], Hikaru NAKAMURA[*2], Taito MIURA[*3]

ABSTRACT

The study focuses on effects of material properties, specifically fracture energy and tensile strength, on corrosion-induced cracking behavior, which are investigated analytically with Rigid Body Spring Method combined with corrosion expansion model. Various material properties are introduced into the analytical model to investigate the influences on crack propagation. The analytical results show that surface crack initiation is determined by tensile strength while the increase of fracture energy will slow down the propagation of surface crack. In addition, it is found that high fracture energy will lead to internal cracks of wide specimen propagating diagonally to concrete surface rather than sides of specimen as those of narrow specimen do, which constrains the final spalling volume. Consequently, it can be identified that ductile materials with high fracture energy is efficient to limit the cracking damage on concrete caused by rebar corrosion.

Keywords: Fracture Energy, Corrosion, Cracking, Spalling Volume, RBSM

1. INTRODUCTION

Deterioration of reinforced concrete structures due to internal rebar corrosion has become a big concern for the durability of structures. Generated corrosion products occupy larger volume than original rebar, imposing expansive stress on the surrounding concrete. Once the expansive stress exceeds the tensile strength of concrete, the cracking initiate, which indicates that concrete cover cracking is highly in relation with the material properties. Experimental studies in literatures [1] and [2] involved with material properties were to investigate the influence of water-cement ratio on crack development rather than fracture energy or tensile performance, since they can be hardly used as test variables. On the other hand, several analytical methods have been developed to simulate crack propagation due to rebar corrosion [3] and [4]. Our lab also proposed a method based on three-dimensional Rigid Body Spring Method (RBSM), which is a kind of discrete numerical methods and can describe crack development accurately [5]. When this sophisticated simulation method is applied, it presents the realistic cracking behavior and is also convenient to study several influencing factors. Moreover, the clarification of these impacts will be beneficial to repair work, since it gives judgments on the efficiency of high strength material or high ductile material on cracks repairing

In this study, Rigid Body Spring Method combined with corrosion expansion model to simulate the corrosion-induced concrete cracking is verified initially through comparing to experimental data in terms of crack width development and crack patterns, which are obtained from accelerated corrosion tests of normal concrete specimens in variety of specimen dimensions [6] and [7]. Then different material properties are introduced into the analytical model to study influences of fracture energy and tensile strength on cracking behavior, in which various geometric features of specimens including specimen width and cover thickness are also taken into consideration.

2 ANALYTICAL METHOD [5]

2.1 Three-dimensional RBSM

RBSM employs a discrete numerical analysis approach. This method represents a continuum material as an assemblage of rigid particle elements interconnected by zero-length springs along their boundaries, which is depicted in Fig. 1. In this study, three dimensional RBSM was applied [8]. The elements are randomly generated with Voronoi Diagram, each of which has six freedom degrees at the center points of triangles formed by the center and vertices of the boundary between two elements. At each center point of these triangles, three springs, one normal and two shear springs are set. As crack widths can be automatically calculated during analysis, it is convenient to simulate concrete cracking process with this method.

2.2 Material Models

Fig. 2 shows the material models of concrete

*1 Graduate School of Engineering, Nagoya University, JCI Student Member
*2 Professor, Dept. of Civil Engineering, Nagoya University, Dr.E., JCI Member
*3 Assistant Prof., Dept. of Civil Engineering, Nagoya University, JCI Member

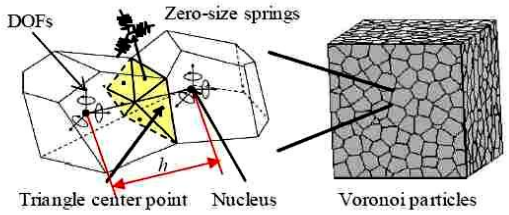

Fig. 1 Voronoi particle definition of RBSM element

applied in analysis. Tensile and compressive models are introduced into normal springs, where f_t represents tensile strength, G_F tensile fracture energy, h distance between centers of Voronoi elements, f_c' compressive strength, G_{Fc} compressive fracture energy and E Young modulus. Shear model is introduced into shear springs, in which the shear strength is assumed to follow the Mohr-Coulomb type criterion with the tension and compression caps.

Besides, the shear transferring capacity at the cracked interface changes based on the crack opening. In order to take into consideration this effect, the shear stiffness is reduced by using a function of the strain normal to the crack as shown in the shear-reduction model in Fig. 2b, where G is the shear stiffness.

Rebar is modeled as linear elastic in the analysis with the Young modulus of 200GPa.

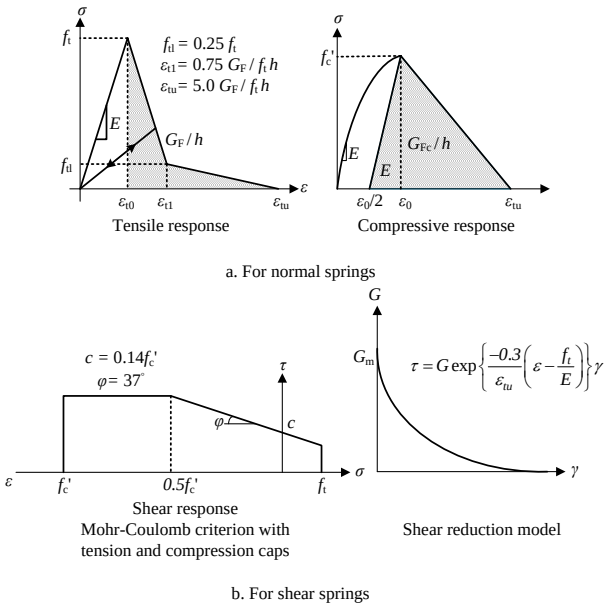

Fig. 2 Concrete material model

2.3 Corrosion Expansion Model

Expansion of corrosion products caused by rebar corrosion inside concrete was modeled by internal expansion pressure as explained in Fig. 3 In this method, a three-phase material model including rebar, corrosion products and concrete was applied. Expansion pressure was modeled with increment of initial strain applied on the boundary between corrosion product layer and rebar layer, which was calculated by equation (1) [9]:

$$\Delta\sigma_{cor} = E_r\left(\Delta\varepsilon - \Delta\varepsilon_0\right) = E_r\left(\frac{\Delta U_{cor}}{H} - \frac{\Delta U}{H}\right) \quad (1)$$

Where,

E_r : elastic modulus of rust

ΔU_{cor} : increment of real increase of rebar radius

ΔU : free increase of rebar radius

H : thickness of corrosion product layer

It is noted that rebar is much more corroded in the part surrounded by cracked concrete or concrete with only minor cracks. In consideration of relative influences of rebar local corrosion in radial direction, increment of initial strain was only applied over one quarter of the model as described in Fig. 3 when a vertical crack near rebar exceeding 0.1mm in width.

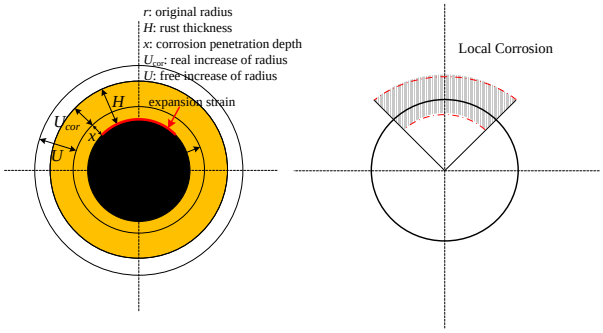

Fig. 3 Corrosion expansion model

It has been reported that corrosion products will penetrate into the formed cracks during rebar corrosion process, which in turn reduces the internal expansion pressure caused by rebar corrosion and retards the crack propagation [10]. In order to allow for this effect in the corrosion expansion model, effective increment of the free increase ΔU_{eff} based on the reduction of volume of corrosion products that are accommodated in cracks with a width larger than 0.1mm was employed. The increment value for an analysis step was determined as follows and also explained in Fig. 4.

$$\Delta U_{\text{eff}} = \Delta U - \frac{\Delta V_{\text{crk}}}{2\pi \cdot r \cdot L} \quad (2)$$

Where,

ΔV_{crk} : increment of volume of accommodated rust

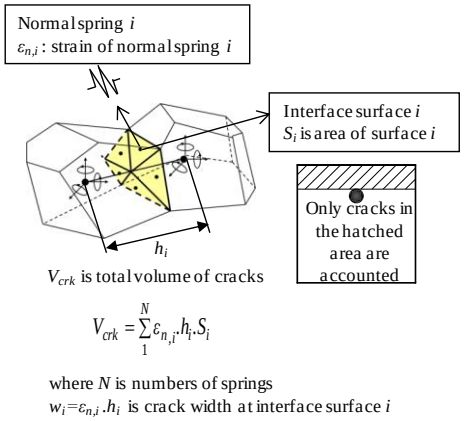

Fig. 4 Calculation of volume of cracks accommodating corrosion products

3. COMPARISON OF ANALYTICAL AND EXPERIMENTAL DATA

The applicability of employed analytical method to simulate crack development of normal concrete specimens due to rebar corrosion is verified by comparing the numerical results with the experimental measurements.

Simulated corrosion tests were performed in our lab in order to study corrosion-induced concrete cracking behaviors when rebar was corroded uniformly in longitudinal direction [6] and [7]. During experiments, rectangular single-rebar specimens with various dimensions were subjected to accelerated corrosion tests to study the effects of specimen size on crack initiation and propagation. One deformed steel bar with a diameter of 19mm was embedded in each specimen with a cover thickness of 30mm. The conduction time was varied for all specimens to investigate crack patterns and crack width development under different corrosion degrees. A description of test variables is listed in Table 1 and specimen dimensions are illustrated in Fig. 5. After each accelerated corrosion test completed, surface crack width was measured and the specimen was cut afterwards for the observation of internal crack patterns and measurement of internal crack widths and lengths.

Table 1 Corrosion test variables

Specimen	Width (mm)	Height (mm)	Length (mm)	f_c (MPa)	Corrosion amount (mg/cm^2)
W150	150	150	300	18.5	26,58,108,162 175,198,445,915
W300	300	150	200	28.0	289,551,882
W400	400	400	200	28.0	147,167,560,1014

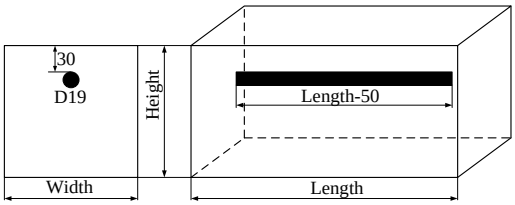

Fig. 5 Specimen dimensions

Table 2 Material parameters in analytical models

Specimen	E (GPa)	f_t (MPa)	f_c (MPa)	G_F (N/m)
W150	30.3	1.53	25.9	35.6
W300,W400	39.2	2.22	39.2	42.2

For comparison, RBSM models with the same dimensions as test specimens were created. The material parameters employed in analytical models are listed in Table 2.

In Fig. 6, the simulated surface crack width developments are compared to the experimental data. It can be seen that the analytical results are in good agreements with the experimental results, not only in the crack width values, but also in the propagation tendency, i.e. the surface crack initiates at the corrosion amount of approximately 50mg/cm^2 and then propagates quickly. Due to the impacts of corrosion products penetrating into cracks, the speed of surface crack propagation is reduced afterwards. It is noted that both experimental and analytical results show that surface crack width has an evident increase when specimen width reduced，which is caused by the enlarged vertical deformation of concrete cover and increased surface bending stress due to the limitation of deformation along the width direction [6].

Fig. 7 displays comparisons of the analytical lateral crack lengths and experimental results. In simulation, lateral crack length was computed from the side of the rebar to the tip of a visible lateral crack, i.e. the crack width was larger than 0.1mm. As can be seen, the analytical results appear similar to the experimental data. Both results show lateral crack length will converge to a certain value rather than continue to increase when corrosion amount exceeds 400 mg/cm^2.

Comparisons of modeled internal crack patterns and those observed in corrosion tests are presented in Fig.8, where the red signs in analytical results represent the cracks with a width of 0.1mm and over. It is shown that the modeled crack pattern corresponds well to the experimental observations. The internal crack patterns of W300 series from experiments are slightly different from other series and also analytical results that lateral cracks incline to concrete surface. It is likely to be affected by a different corrosion state and the distribution of coarse aggregates near reinforcement.

It is confirmed that the analytical method can simulate corrosion-induced concrete crack propagation accurately with various geometric features of specimens.

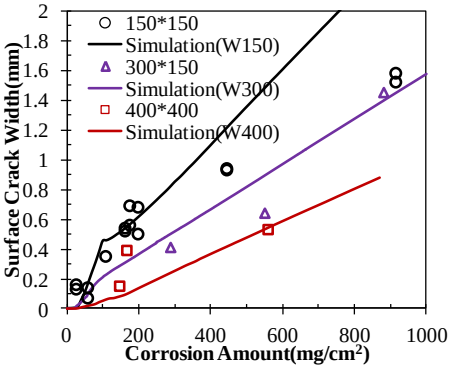

Fig. 6 Comparisons of surface crack width development

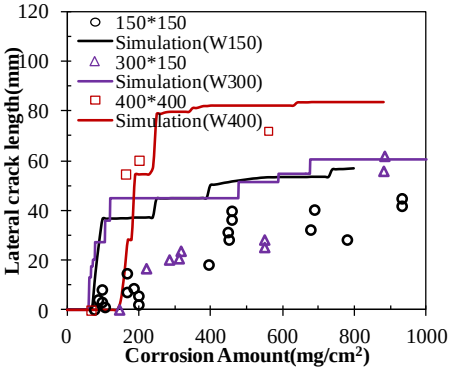

Fig. 7 Comparisons of lateral crack length

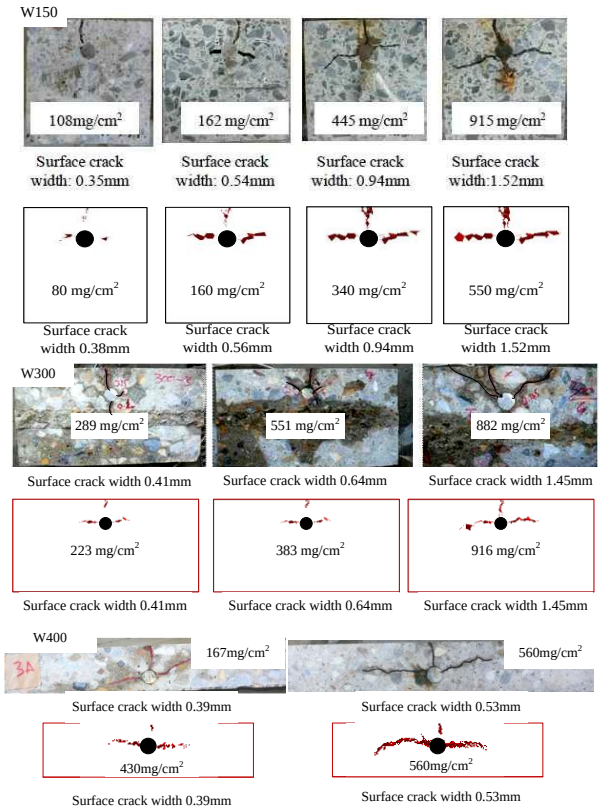

Fig. 8 Comparisons of internal crack patterns

4. INFLUENCE OF MATERIAL PROPERTIES ON CRACK DEVELOPMENT

4.1 Analysis Outline

In this part, the validated analytical method by comparing to corrosion test results of normal concrete specimen was employed to investigate the influences of material properties on corrosion-induced cracking behavior, which contributed to clarify the efficiency of repairing materials with high tensile strength or high ductility on the maintenance of reinforced concrete structures suffering from severe internal rebar corrosion. One of the advantages of RBSM model is that different material properties can be modeled with reasonable parameters as shown in Fig. 9. The two groups of material properties were obtained by tension simulation with the same mesh size as subsequent investigation of effects of material properties. In the first group, tensile strength has a range of 2.22 to 6.43MPa while fracture energy stays the same as 84.3N/m. In the other group, fracture energy is increased from 84.3 to 3063N/m while the tensile strength is kept as 2.22MPa.

The effect of penetration of corrosion products into cracks was neglected in this analysis, since this effect rendered few influences on crack patterns, compared with the impacts of local corrosion, and it could also reduce the computation complexity.

Single-rebar specimens with a rebar diameter of 19mm were studied. The dimensions of created specimens are in accord with the one as described in Fig. 5, in which specimen width varies as 150, 300 and 600mm and the cover thickness is change from 10 to 30mm simultaneously. The created RBSM model is shown in Fig. 10.

4.2 Surface crack development

Fig.11 shows surface crack propagation for different tensile strengths. As can be seen, corrosion amount corresponding to surface crack initiation increases with tensile strength. However surface crack width propagates following nearly the same route after initiation. Although surface crack generation is retarded by high tensile strength, a bigger crack opening will appear conversely and then expand rapidly. It can be deduced that surface crack propagation is not related with tensile strength.

Surface crack development for different fracture energies is presented in Fig. 12. In general, it can be seen that regardless of various geometric features, surface crack width decrease obviously when fracture energy increases. Compared with impacts of tensile strength, it seems that surface crack propagation is controlled by fracture energy while tensile strength is dominant in crack initiation. Thus, ductile materials with high fracture energies can be used to control surface crack development for maintenance of cracked concrete due to rebar corrosion.

In comparison of the corrosion amounts corresponding to surface crack initiation between different cover thicknesses, it can be seen that crack appearance is delayed by an increase of cover thickness.

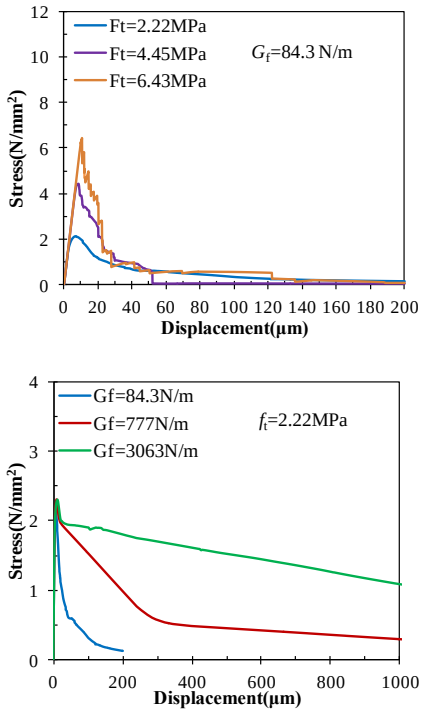

Fig. 9 Stress-displacement relationship of analytical specimens

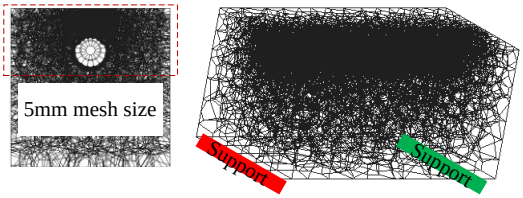

Fig. 10 RBSM model

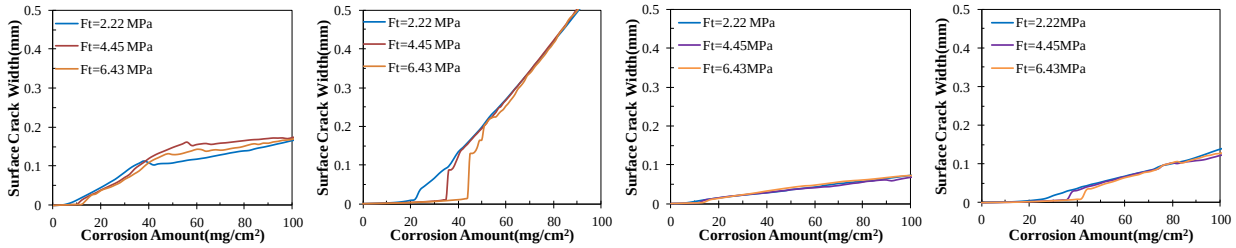

a) C10W150 b) C30W150 c) C10W600 d) C30W600

Fig. 11 Surface crack development for various tensile strengths

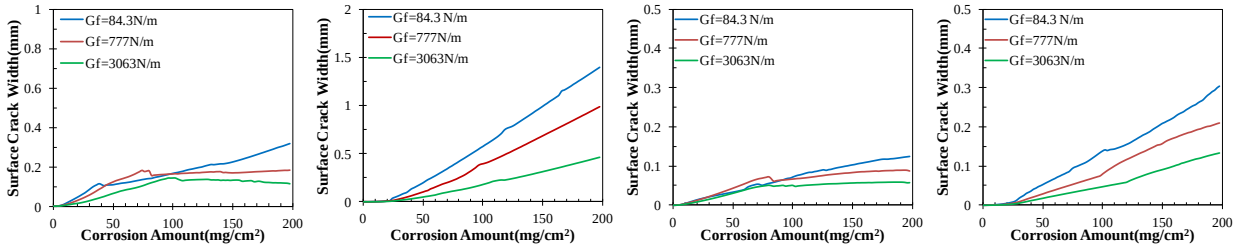

a) C10W150 b) C30W150 c) C10W600 d) C30W600

Fig. 12 Surface crack development for various fracture energies

In addition, the smaller cover thickness, the smaller surface crack width, which can be attributed to the differences in internal crack patterns, i.e. the lateral cracks inside concrete becomes dominant when cover thickness is reduced.

Regarding specimen width, it appears that surface crack initiation is independent of specimen width. And increasing the specimen width can result in the reduction of surface crack width.

4.3 Internal crack propagation

For normal material properties, the internal crack patterns remain the same in spite of different specimen widths as shown in Fig. 8. However in the case of high fracture energy, internal crack pattern becomes in relation with the specimen width. The internal crack patterns of the specimens with a cover thickness of 10mm were almost the same and irrelevant to specimen width even if fracture energy was increased. Therefore, only results with regard to 30mm cover thickness are discussed as follows.

Fig. 13 displays internal crack patterns corresponding to corrosion amount of 70mg/cm^2, 100mg/cm^2 and 140 mg/cm^2 separately for specimen width of 150mm. In this case, various fracture energies result in the same crack pattern, i.e. lateral cracks develop toward sides of specimen along with vertical crack propagating from surface to rebar. The influence of fracture energy is merely that crack propagation becomes slow.

Fig. 14 presents internal crack pattern of specimen with a width of 600mm under the corrosion amount of 100, 140 and 170 mg/cm^2 separately. It can be found that high fracture energy leads to lateral cracks developing diagonally toward concrete surface. Besides, lateral crack length decreases evidently with an increase of fracture energy as shown in Fig. 15. It is identified that ductile materials with high fracture energy used in repair will constrain cracked areas and thereby reduce the spalling area of reinforced concrete slab specimen.

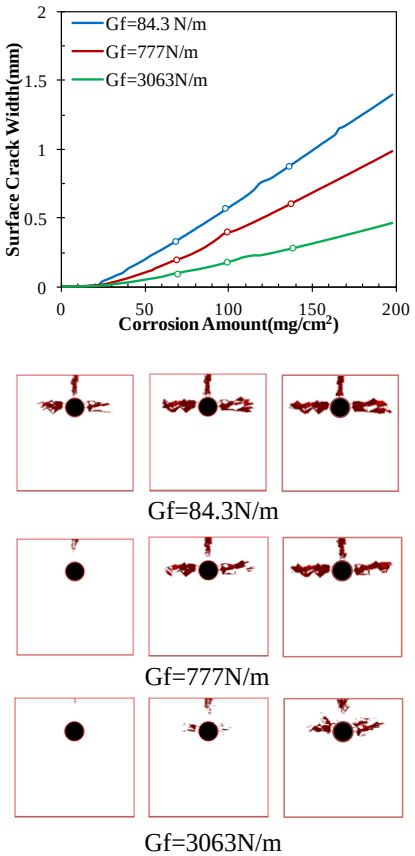

Fig. 13 Internal crack patterns of specimen with a width of 150mm

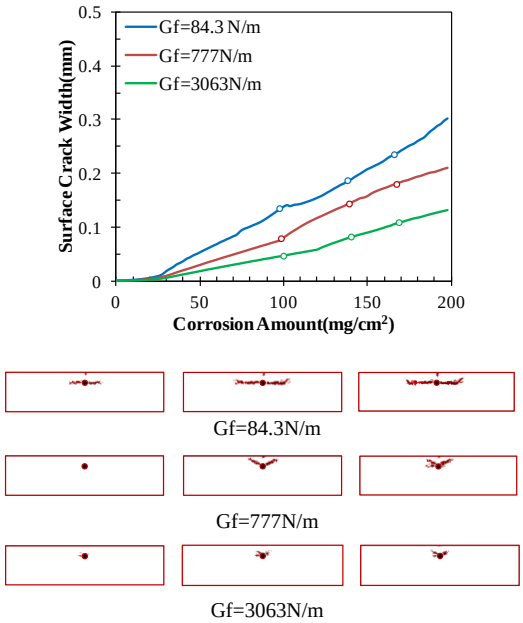

Fig. 14 Internal crack patterns of specimen with a width of 600mm

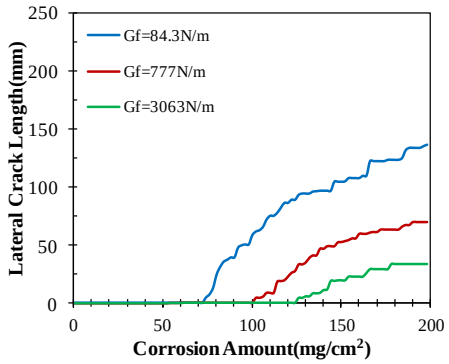

Fig. 15 Lateral crack length of specimen with a width of 600mm varied in fracture energy

5. CONCLUSIONS

Generally, it can be concluded from the current study that:

(1) The ability of three dimensional RBSM model combined with corrosion expansion model to evaluate the cracking behavior of normal concrete caused by rebar corrosion was verified through comparing to accelerated corrosion test results for various specimen dimensions. There is a good agreement between the analytical results and experimental data in terms of surface crack width, lateral crack length and internal crack patterns.

(2) The analysis to investigate the effects of material properties on corrosion-induced cracking behavior with confirmed numerical model shows that surface crack initiation is determined by tensile strength while fracture energy imposes a significant influence on surface crack propagation.

(3) For wide specimen, the increase of fracture energy will result in internal cracks propagating diagonally toward concrete surface and reduce the spalling volume of concrete cover.

(4) The effectiveness of ductile materials owing high fracture energy on restricting the surface crack development is identified. In addition, it will be beneficial to reducing spalling area of concrete slab in danger of significant rebar corrosion.

REFERENCES

[1] Alonso, C. et al.,"Factors Controlling Cracking of Concrete Affected by Reinforcement corrosion," Materials and Structures, Vol. 31, 1998, pp. 435-441.

[2] Vu, K., Stewart, M. G., and Mullard, J.,"Corrosion-induced Cracking: Experimental Data and Predictive Models," Journal of ACI Structure, Vol. 102, 2005, pp. 719-726.

[3] Chernin, L., Val, D. V., and Volokh, K. Y.,"Analytical Modelling of Concrete Cover Cracking Caused by Corrosion of Reinforcement," Materials and Structures, Vol. 43, 2010, pp. 543-556.

[4] Chen, D., and Mahadevan, S.,"Chloride-induced Reinforcement Corrosion and Concrete Cracking Simulation," Cement and Concrete Composites, Vol. 30, 2008, pp. 227-238.

[5] Tran, K. K. et al.,"Analysis of Crack Propagation due to Rebar Corrosion Using RBSM," Cement and Concrete Composites, Vol. 33, 2011, pp. 906-917.

[6] Kawamura, K. et al.,"Experimental Investigation of Surface and Internal Cracks Propagation due to Rebar Corrosion," Proceeding of JCI Annual Convention., JCI, Vol. 32, 2010, pp. 1007-1012, (in Japanese).

[7] Tran, K. K.," Study on Cracking Behavior of Concrete due to Rebar Corrosion," Doctor Thesis. Nagoya University, 2012, pp. 190-210.

[8] Yamamoto, Y. et al.,"Analysis of Compression Failure of Concrete by Three Dimensional Rigid Body Spring Model," Doboku Gakkai Ronbunshuu, Vol. 64, 2008, pp. 612-630, (in Japanese).

[9] Lundgren, K.,"Modeling the Effect of Corrosion on Bond in Reinforced Concrete," Magazine Concrete Research, Vol. 54, 2002, pp. 359-374.

[10] Val, D. V., Chernin, L., and Stewart, M. G.,"Experimental and Numerical Investigation of Corrosion-induced Cover Cracking in Reinforced Concrete Structures," Journal of Structural Engineering., ASCE, Vol. 135, 2009, pp. 376-385.